LAWRENCE
LIVERMORE
NATIONAL
LABORATORY

UCRL-JRNL-200602

Chemically Transformable Configurations of Mercaptohexadecanoic Acid Self-Assembled Monolayers Adsorbed on Au(111)

T. M. Willey, A. L. Vance, T. van Buuren, C. Bostedt, A. J. Nelson, L. J. Terminello, C. S. Fadley

October 28, 2003

Langmuir

Chemically Transformable Configurations of Mercaptohexadecanoic Acid Self-Assembled Monolayers Adsorbed on Au(111)

Trevor M. Willey[1,2], Andrew L. Vance[2], T. van Buuren[2], C. Bostedt[2], A. J. Nelson[2], L. J. Terminello[2], and C. S. Fadley[1,3]

[1]University of California, Davis, CA 95616

[2]Lawrence Livermore National Laboratory, Livermore, CA 94551

[3]Lawrence Berkeley National Laboratory, Berkeley, CA 94720

January 13, 2004

Abstract

Carboxyl terminated Self-Assembled Monolayers (SAMs) are commonly used in a variety of applications, with the assumption that the molecules form well ordered monolayers. In this work, NEXAFS verifies well ordered monolayers can be formed using acetic acid in the solvent. Disordered monolayers with unbound molecules present in the film result using only ethanol. A stark reorientation occurs upon deprotonation of the endgroup by rinsing in a KOH solution. This reorientation of the endgroup is reversible with tilted over, hydrogen bound carboxyl groups while carboxylate-ion endgroups are upright. C1s photoemission shows that SAMs formed and rinsed with acetic acid in ethanol, the endgroups are protonated, while without, a large fraction of the molecules on the surface are carboxylate terminated.

1 Introduction

Surface modification by using ω-functionalized alkanethiols is the most simple way to create flat, chemically or biologically functionalized surfaces. Often, well ordered monolayers of molecules beyond alkanethiols with such functionalizations are non-trivial to achieve.[1,2]

Carboxyl terminated Self-Assembled Monolayers (SAMs) are the basis for chemically and biologically functionalized surfaces. Often this type of SAM is used as a starting point for fabricating biologically active surfaces in order to immobilize proteins or other biological agents for further analysis.[3,4] Carboxylate terminated SAMs have also recently been mechanically and conformationally switched on a surface.[5] The molecules were deposited in dilute fashion on a surface and the carboxylate endgroup was electrochemically pushed toward or away from the electrode with the associated conformational and hydrophilic to hydrophobic surface property changes. Understanding of biological molecules attached to SAMs and molecular mechanically switching devices require a fundamental understanding of how these monolayers form, and their conformations upon formation.

Results have varied on the structure of carboxyl terminated SAMs. One of the first comprehensive studies of the structure and formation of mercaptohexadecanoic acid adsorbed on Au(111) observed well-packed self-assembled monolayers through the sharpness of FTIR CH_2 stretching peaks and determined the the chains had a tilt-angle similar to that of alkanethiols through their relative intensities.[6] This study also found the polar angle of the carbonyl bond to be about 66^o from normal with the OH group exposed to the surface. Subsequent, Near-Edge X-ray Absorption Fine Structure (NEXAFS) measurements showed a high degree of disorder in these films.[7,8] However, recent FT-IR studies, with a strict protocol for SAM preparation, confirm the ordering in these SAMs that is highly dependent on the state of the carboxyl group.[9]

In this paper, ordering in carboxyl terminated SAMs under the proper preparation conditions of a solution containing acetic acid is verified with NEXAFS and the orientation of the carboxyl plane is determined. These monolayers are compared to those prepared with the standard protocol of dissolving the SAM precursors in ethanol only. This work reports the first observation of stark conformational changes occur in the end-group upon deprotonation to

carboxylate.

2 Experimental

2.1 Reagents and Materials

Reagents were purchased from commercial sources and used as received. 16-mercaptohexadecanoic acid (90%), hexadecanethiol (95%) and ethanol (99.9%) were purchased from Aldrich. Acetic acid (HPLC grade, 99.7%) was purchased from VWR. Au(111) substrates were formed by evaporating 5 nm Ti and then 100nm Au on Si(100) under high vacuum. All gold substrates were hydrogen flame annealed immediately before use.[10]

2.2 Sample Preparation

Solutions were prepared as per Arnold et al.[9] by dissolving mercaptohexadecanoic acid into 5% (by volume) acetic acid/ethanol to reach the desired concentrations between 1μmol and 1mmol. The ethanol only sample and corresponding methyl terminated SAM were prepared by diluting the mercaptohexadecanoic acid into ethanol. Gold substrates were placed in these solutions for 24-36 hours. Each sample was then removed, rinsed with its pure solvent: 5% acetic in ethanol for samples formed in 5% acetic/ethanol, or pure ethanol for samples made without acetic acid in solution. Samples were immediately introduced into ultra-high vacuum. The samples presented here for acetic/ethanol prepared SAMs were formed concurrently under the same ambient conditions.

2.3 Instrumentation

X-ray absorption spectra were taken at VUV BL 8.2 of The Stanford Synchrotron Radiation Laboratory (SSRL,SPEAR II) at the Stanford Linear Accelerator Center. The beamline uses bend magnet radiation and a spherical grating monochromator.[11] XAS experiments were conducted with an energy resolution of $\sim$0.2 eV at the carbon K-edge. Absorption spectra were recorded simultaneously using both total electron yield (TEY) and auger electron yield

(AEY). The measured total current leaving the sample constitutes TEY. AEY measurements consists of measuring the intensity of the appropriate auger electron at a given fixed kinetic energy while scanning the X-rays through the absorption edge. Both currents were normalized to the incident beam via the current from a clean grid with a freshly evaporated gold coating. Care was taken to limit x-ray flux to minimize damage to the samples during data collection.[12] All spectra were recorded at a base pressure of less than 1 x 10^{-9} torr. With E_p the component of the electric field in the plane of incidence and E_s the component perpendicular to the plane, the degree of linear polarization P, defined as

$$P = \frac{{E_p}^2}{{E_s}^2 + {E_p}^2} \tag{1}$$

was measured with highly-oriented pyrolytic graphite (HOPG.) The polarization was measured by rotating about two different axes such that the intensity of the C 1s to π^* feature in the C K-edge spectra indicated the relative magnitudes of ${E_p}^2$ and ${E_s}^2$. A few days prior to these measurements, this method measured the polarization at ~88% in the plane of the storage ring. The energy scale of carbon XAS spectra were calibrated to the π^* resonance of HOPG set to 285.38 eV.[13]

X-ray photoelectron spectra were obtained at SSRL using a PHI 15-255G CMA electron energy analyzer and its associated OEM electronics. The pass energy was set to 25 eV for XPS spectra. S2p spectra were obtained at a photon energy of 280eV; C1s spectra were obtained at a photon energy of 400eV. The spectra were not normalized to the beam current. Spectra of the Au4f peaks of the substrates were taken immediately after each sulfur and carbon spectrum to calibrate the binding energy scales. The Au $4f_{7/2}$ photoelectron at 84.01 ± 0.05 eV was used to convert the kinetic energy scales to binding energy scales.

FTIR spectra were obtained using a Nicolet 560 FTIR with an MCT detector and a reflecting grazing incidence accessory. The largest aperture was used (1.7cm x 2.7cm) for analysis, and either freshly H_2 flame annealed gold substrates or SAMs consisting of undecanethiol on gold were used as a background reference.

2.4 Analysis

NEXAFS quantitatively determines the orientation of bonds through polarization dependencies of various resonances. One can then determine the orientation of the alkyl chains and the carboxyl groups terminating the molecules. The intensity of a resonance is proportional to the dot product of the electric field vector and the transition dipole moment. For these SAMs, the Au(111) substrate has threefold azimuthal symmetry. The transition dipole moment can be modeled as a vector in the case of the C-C σ^* molecular orbitals along C-C backbone of the alkyl chain or the π^* orbital whose transition dipole moment vector is perpendicular to the O=C-O plane. The intensity I for the vector case is:[14,15]

$$I_v(\theta,\alpha) \propto \frac{1}{3}P\left(1+\frac{1}{2}\left(3\cos^2\alpha-1\right)\left(3\cos^2\theta-1\right)\right)+\frac{1}{2}(1-P)\sin^2\alpha \tag{2}$$

where θ is the angle between the incident radiation and the surface, α is the angle between the surface normal and the transition dipole moment vector, and P is the polarization of the beam in the plane of incidence defined in eqn. 1. One can also model the transition dipole moment as a number of resonances in a given plane as in C-H σ^* like Rydberg R* resonances[16] or the two C-O σ^* bonds in the O-C=O plane of the carboxyl group. For orbitals in a plane, the intensity is:[14,15]

$$I_p(\theta,\gamma) \propto \frac{2}{3}P\left(1-\frac{1}{4}\left(3\cos^2\theta-1\right)\left(3\cos^2\gamma-1\right)\right)+\frac{1}{2}(1-P)\left(1+\cos^2\gamma\right) \tag{3}$$

where θ is again the angle between the incident radiation and the surface, P is the polarization, and γ is the angle between the normal to the transition dipole moment plane and the normal to the surface.

To remove the proportionality, ratios are taken between spectra taken at different incident angles. In order to greatly simplify analysis, the intensities are left as functions of cosine squared, with $\Theta = \cos^2\theta$, $A = cos^2\alpha$, and $\Gamma = cos^2\gamma$ the intensities from equations 2 and 3 become:

$$\frac{I_v\left(\Theta_i,A\right)}{I_v\left(\Theta_j,A\right)} = \frac{P\left(3A-1\right)\Theta_i - A + 1}{P\left(3A-1\right)\Theta_j - A + 1} \tag{4}$$

and

$$\frac{I_p\left(\Theta_i,\Gamma\right)}{I_p\left(\Theta_j,\Gamma\right)}=\frac{P\left(3\Gamma-1\right)\Theta_i-\Gamma-1}{P\left(3\Gamma-1\right)\Theta_j-\Gamma-1} \tag{5}$$

These two equations are linear in Θ_i. A linear regression is then obtained from all spectra acquired at Θ_i vs. each incidence spectrum taken at Θ_j. One can then solve for α, γ as a function of the slopes and/or offsets.

Another common method of determining orientation of bonds is through taking the difference of spectra taken at various incidence angles and comparing to a sample of a known orientation.[15] As a function of $\cos^2(\theta_i)-\cos^2(\theta_j)$ (or $\Theta_i-\Theta_j$) these equations are also linear:

$$I_v\left(\Theta_i,A\right)-I_v\left(\Theta_j,A\right)=SP\left(\frac{3}{2}A-\frac{1}{2}\right)\left(\Theta_i-\Theta_j\right) \tag{6}$$

$$I_p\left(\Theta_i,\Gamma\right)-I_p\left(\Theta_j,\Gamma\right)=SP\left(-\frac{3}{2}\Gamma+\frac{1}{2}\right)\left(\Theta_i-\Theta_j\right) \tag{7}$$

so linear regressions of all difference spectra taken at Θ_i and Θ_j can be made to to determine angles relative to a sample with a known orientation to determine S, the transition dipole moment cross section, and P the polarization.[15]

Using regressions on a number of spectra, one can obtain a high degree of precision. Typical error bars for precision are less than 1.0^o However, these values of precision do not represent a number of other sources of systematic errors which lead to an estimated accuracy of 4-5^o.

3 Results and Discussion

Changes in the ordering of carboxyl-terminated SAMs were investigated using films prepared in various environments. SAMs were prepared in concentrations of 1μmol to 1mmol with 5% acetic acid in ethanol as the solvent and rinsed in clean solvent. For comparison, SAMs were prepared with only ethanol as the solvent and rinse. Samples were also prepared by using the acetic acid/ethanol solvents and then rinsed in a basic solution (results presented here are a KOH solution, pH 12-13) to investigate how deprotonation affects the SAM. Carbon K-edge absorption spectra

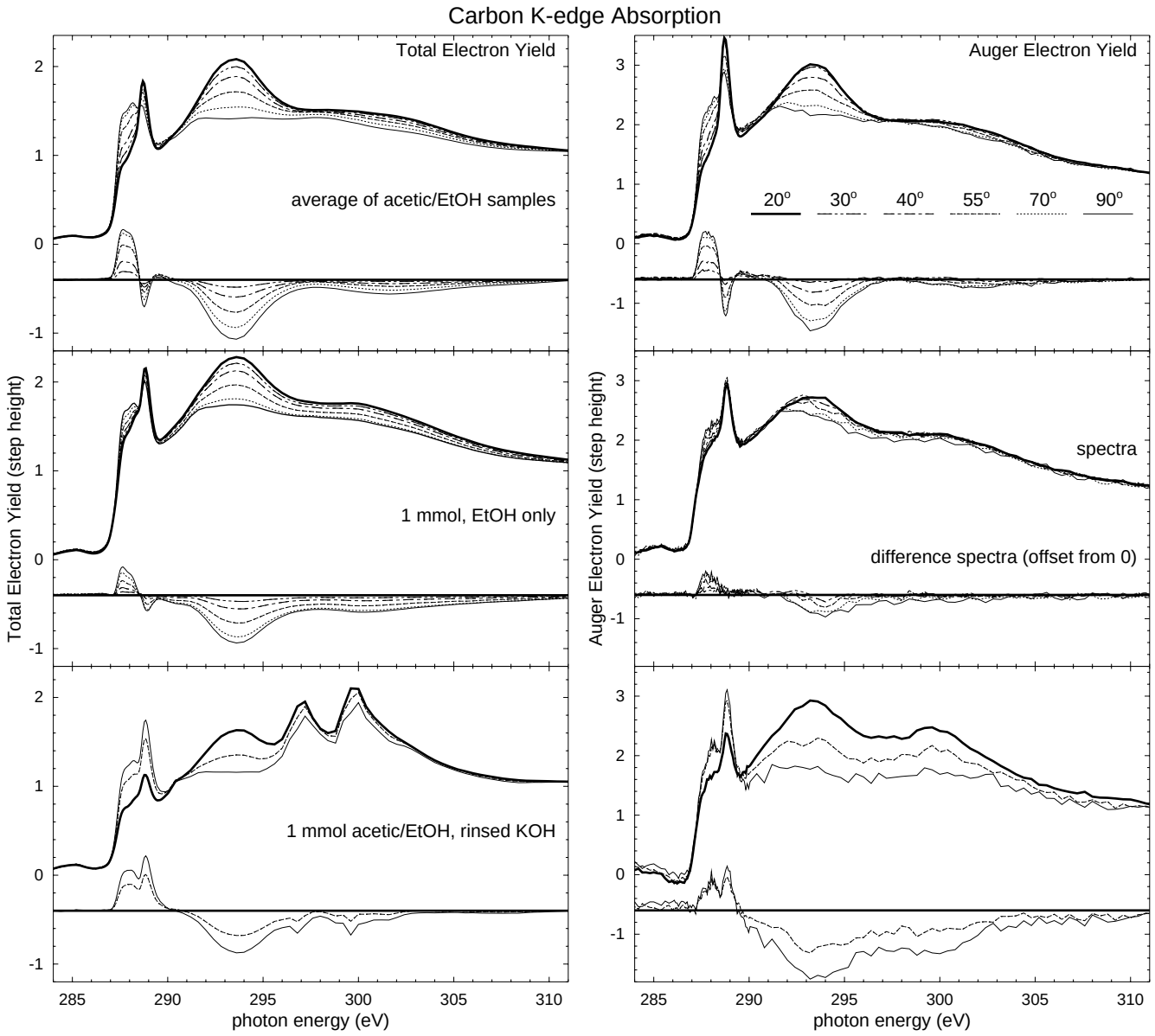

Figure 1: Carbon K-edge total-electron and auger-electron yield absorption spectra and difference spectra. Top panes: average of 0.001, 0.01, 0.1, and 1 mmol samples formed and rinsed in acetic acid / ethanol. Middle panes: 1 mmol sample formed in ethanol only. Lower panes: Sample formed in acetic/ethanol, but then rinsed in KOH; peaks due to K 2p are visible in TEY spectra, and AEY measurements have higher S/N due to shorter acquisition time.

are displayed in figure 1 with total electron yield measurements in the left panes and auger yield in the right panes. The topmost panels are the average of 4 samples (0.001, 0.01, 0.1, and 1 mmol) formed and rinsed in 5% acetic acid in ethanol. Middle panels contain spectra from a sample formed from a solution of 1mmol mercaptohexadecanoic acid in only ethanol. The lower panels contain spectra from a sample formed in acetic acid / ethanol, but later rinsed in a KOH solution. Two features at 297 and 300 eV in the KOH rinsed spectra are due to the K 2p states rather than the carbon in the monolayer. All other features are common to all the spectra. The first two resonances near the ionization potential at 287.65 and 288.10 eV are Rydberg states associated with alkyl (CH_2) chains.[16] The next feature at 288.7eV is a transition into a π^* state of the carboxyl functionalization of the SAM. The two broad features above the edge are primarily C-C σ^* transitions.

Carbon polarization dependencies can be computed using these five resonances which have large intensity changes: the Rydberg like states, which have transition dipole moments along the C-H bonds, the carboxyl π^* feature that has a transition dipole moment perpendicular to the O-C=O plane, and the C-C and C-C'σ^* which have a transition dipole moment along the alkyl chain molecular axis.[16,17] The CH_2 Rydberg and carboxyl π^* resonances overlap and, in many cases have opposite polarization dependencies. This excludes directly using the commonly used difference method to analyze these resonances as the magnitude of the overlapping peaks in difference spectra partially cancel each other. However, deconvolution of these resonances via peak fitting allows accurate determination of the orientation of the molecule. This was accomplished by simultaneously fitting spectra acquired at different incident angles and their difference spectra. Peak positions and widths for each resonance were held constant between spectra while the amplitudes were allowed to vary independently. Peak positions, widths and amplitudes were varied by a Monte Carlo method, and new fit parameters were only accepted if the sum of the square of residuals for all spectra was better with the new parameter.

Table 1 lists angles found through analysis of the polarization dependencies. Alkyl R*, σ^*, and carboxyl π^* were found using the slopes and offsets of regressions from equations 4 and 5, while angles found through equations 6 and 7 are listed diff. R*, diff σ^*, and diff. π^*. Few differences occur between the SAMs formed in acetic acid solutions,

Table 1: Carbon tilt angles between alkyl chain (or O-C=O plane) and sample normal for all samples.

	.001mmol	.01mmol	.1mmol	1mmol	EtOH	KOH
alkyl R*	39.9	39.7	40.0	38.4	48.4	39.1[b]
diff. R*	39.9[a]	40.2	41.2	39.8	46.8	[b]
alkyl σ*	41.6	41.1	39.1	38.0	46.9	[b]
diff. σ*	41.6[a]	41.8	38.2	34.7[c]	36.0[c]	[b]
carboxyl π*	44.6	45.5	44.2	44.5	52.1	71.6[b]
diff. π*	44.6[a]	45.0	43.8	44.9[a]	48.6	[b]

[a] used as reference for difference spectra
[b] KOH rinsed sample tilts from C K-edge unavailable
[c] diff. σ* underestimates tilt due to thicker layers in 1mmol, EtOH samples

with a possible slight decrease in polar angle of the alkyl chains with increasing concentration. The carboxyl group is tilted over such that the polar angle of the vector perpendicular to the O-C=O plane is roughly 45-degrees from the surface normal. In the case without acetic acid, the angle derived for the O-C=O plane (52 degrees) is approaching the magic angle, indicating randomly oriented carboxyl groups. In this case, the alkyl chain is also significantly less ordered with a tilt angle of on average 47-8 degrees. In additional samples prepared without acetic acid, alkyl-chain results were irreproducible but generally less ordered than samples prepared with acetic acid. In the KOH rinsed sample, the edge from the potassium 2p appear just above the carbon edge and make normalization of the spectra difficult. However, these spectra in figure 1 indicate a polarization dependence for the carboxyl group that is opposite that of the acetic acid rinsed SAMs, estimating roughly 70^o between the carboxyl plane and sample normal, indicating a reorientation of the end-group. Analysis of oxygen K-edge absorption spectra determine this angle as well as confirm tilt angles found with carbon spectra.

Oxygen K-edge auger-electron yield absorption spectra are displayed in figure 2, and calculated orientational angles presented in table 2. For these samples, auger yield was advantageous and chosen over TEY because of the much better signal to background ratio and enhanced surface sensitivy. However, auger-yield also has its disadvantages in a lower signal to noise ratio, and the possibility that low binding-energy photoelectrons could sweep through the kinetic energy window of the analyzer and hence exist in the spectra. The analyzer was set on the oxygen auger peak and such that Au 4f photoelectron peaks appear well above the absorption edge, while Au valence photoelectron peaks are well below the absorption onset. Unfortunately and unavoidably, the much weaker Au 5p electrons contribute

slightly to the intensity of the O K-edge absorption spectra at ∼566eV. Also, K photoelectrons appear in the spectra rinsed in KOH.

All Oxygen spectra have 1 or 2 pre-edge features at 535eV - 537eV. The first is assigned to transitions from the O1s into π^* orbitals of the carboxyl group. The second feature at 537eV is attributed to a small amount of extra acetic acid left on the surface as it appears only in samples that have been exposed to acetic acid. The broad feature just above the edge from 540-553eV is assigned to a σ^* orbital between the C and O atoms.) The third feature centered about 566eV from 561eV - 574eV has intensity contributed from both another σ^* feature and the Au 5p photoelectrons that have entered the window of the kinetic energy of the analyzer.

The top pane of figure 2 depicts O K-edge polarization dependencies of samples prepared with 1mmol to 1μmol of mercaptohexadecanoic acid in 5%acetic/ethanol. All have polarization dependence with the π^* feature largest at grazing incidence and the σ^* feature largest at normal incidence, indicating the normal to the carboxyl group is tilted about 45° from the substrate normal.

The middle pane of figure 2 shows the polarization dependence of a sample that did not have acetic acid present during the formation or rinsing of the SAM; it lacks the polarization dependence of the previous samples. The angles calculated and listed in table 2 (50.8^o - 51.9^o) approach the magic angle of $\arcsin(\sqrt{2/3})$, indicating a large distribution of orientations for the carboxyl groups and a lack of ordering. In samples prepared in this manner, Ca and Na and other ions were observed in the samples in absorption and photoemission spectra indicating carboxylate terminated molecules exist on the surface. The bottom pane of figure 2 shows the polarization dependence of a sample that was prepared in acetic acid, but then was rinsed in a KOH solution. Spurious features appear that are not due to the carboxyl oxygen atoms at 526 and 544 eV. These features are presumably from the K 3p (17eV) and K 3s (33 eV) photoelectrons as well as a small amount of water that now is on the surface seen in FTIR spectra (figure 4). The polarization dependence, with π^* feature most intense at normal incidence, is opposite that of the samples formed with acetic in solution. This π^* feature indicates the normal to the O=C-O plane is on average ≈ 64° from normal meaning the carboxyl groups are "upright." K photoelectrons hinder determining an angle using

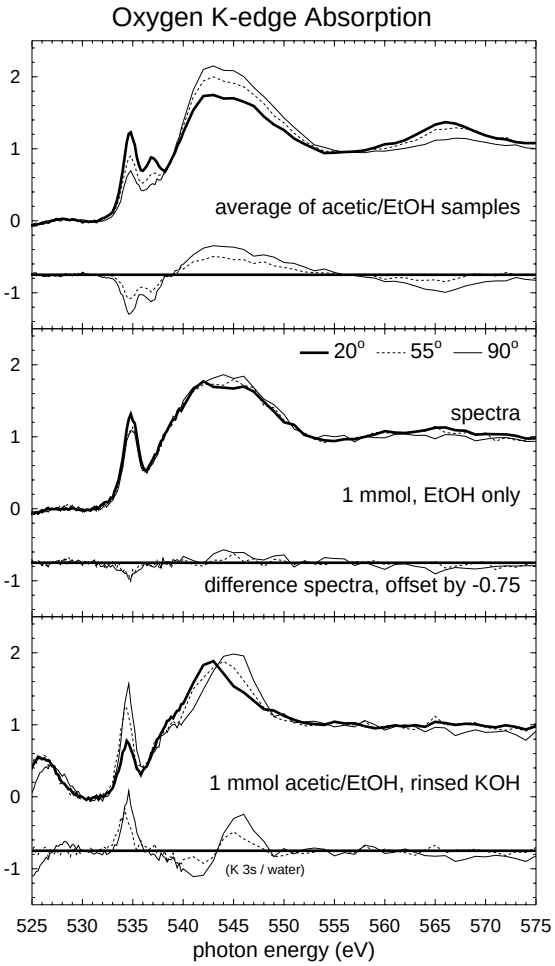

Figure 2: Oxygen K-edge auger-electron yield spectra and difference spectra. The top pane is average obtained from the 1 mmol - 1 μmmol samples, the middle pane spectra are from a 1 mmol sample prepared and rinsed in ethanol only, and the bottom panel spectra are from the KOH rinsed sample.

Table 2: Oxygen tilt angles (between the O-C=O plane normal and sample normal) for all samples.

	.001mmol	.01mmol	.1mmol	1mmol	EtOH	KOH
π^*	45.2	44.6	44.5	46.7	51.9	63.6
diff. π^*	45.2[b]	44.8	45.4	44.7*	51.0	65.5
σ^*	41.6	43.3	40.0	41.6	50.8	[a]
diff. σ^*	41.6[b]	43.5	39.3	45.6	51.4	[a]

[a] σ^* not available on KOH rinsed sample due to K photoelectron peaks

the σ^* resonance of the C-O bonds. This effect is reversible as subsequent protonation returns the endgroup to its previous tilted over state and deprotonation to its upright state, however, data may indicate gradual degradation of the film through multiple rinsings.

The possibility that this effect could be due to odd-even effects was also investigated by comparing the mercaptohexadecanoic acid based SAMs with those formed from mercaptoundecanoic acid.[6] For the mercaptoundecanoic acid based SAM, the tilt of the alkyl chain (42.0°) and carboxyl angle (45.5°) are similar to the angles of the mercaptohexadecanoic acid. This indicates that the orientation of the carboxyl group is not due to odd-even effects and that dimerization of the endgroups is the primary reason for the orientation of the carboxyl group.

In order to further investigate these films and confirm their composition, carbon 1s photoelectron spectroscopy was used. Carbon photoelectron spectra appear in figure 3. The most intense feature in all spectra is due to the alkyl chain of the molecules. The feature completely resolved from this peak at higher energy is due to the endmost carbon atom of the carboxyl group, and this feature is shifted to higher energy due to the electron-withdrawing effect of its binding to two oxygen atoms. The asymmetry of the alkyl peak with intensity to higher binding energy may be due to the carbon atoms near the carboxyl group and/or attributed to recently observed differences in alkyl-chain orbital overlap.[18]

The peak associated with the carbon within the carboxyl group indicates the chemical state of this functionalized surface. This peak is similar for concentrations between 0.001 mmol and 0.1 mmol formed and rinsed in 5% acetic acid in ethanol, with a peak at 289.09-289.15eV, FWHM 1.17-1.25eV. For the 1 mmol sample, the peak is broadened (FWHM 1.60eV) and shifted to lower binding energy at 288.66. The ethanol only sample peak is broadened and shifted even more, with FWHM 1.65eV at 288.48eV, while the KOH rinsed sample exhibits a sharp peak with FWHM

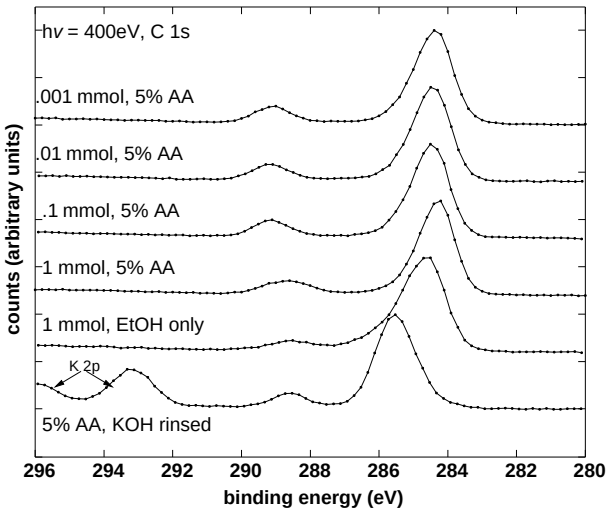

Figure 3: Carbon 1s photoelectron spectra of the series of samples prepared in 5% acetic acid (AA) in EtOH, the sample prepared in only EtOH, and the sample rinsed in KOH.

1.12eV at 288.56eV. This shift to lower binding energy is due to deprotonation of the carboxyl group to carboxylate with the accompanying charge transfer from the cation and screening of the endgroup.

The alkyl peak is asymmetric in the acetic acid/ethanol samples with sharper onset at lower binding energy. In the ethanol only sample, the alkyl peak is broad, likely due to the non-uniform environments the alkyl units experience in this disordered film. In the sample rinsed in KOH, the alkyl peak is shifted to higher binding energy relative to the gold substrate, presumably due to the substrate and alkyl chain screening the K cations at the surface.

This result is also shown in FTIR spectra as seen in figure 4. The SAM formed with acetic acid shows clear carbonyl stretches from 1740-1700cm^{-1}. These have been previously shown to be from single, non-hydrogen bound carboxyl groups at ∼1740cm^{-1}, carboxyl groups hydrogen bound with one hydrogen bond or hydrogen bonds to two different neighboring molecules at ∼1720cm^{-1}, and completely dimerized carboxyl groups with two hydrogen bonds to one neighboring molecule at ∼1700cm^{-1}.[6,9,19] The acetic formed SAMs show a mixture of dimerizations. For the case where the SAM is formed with only ethanol as the solvent, these peaks are reduced, especially those associated with single non-hydrogen bound groups or those with one hydrogen bond. The carboxylate band (1450cm^{-1})is

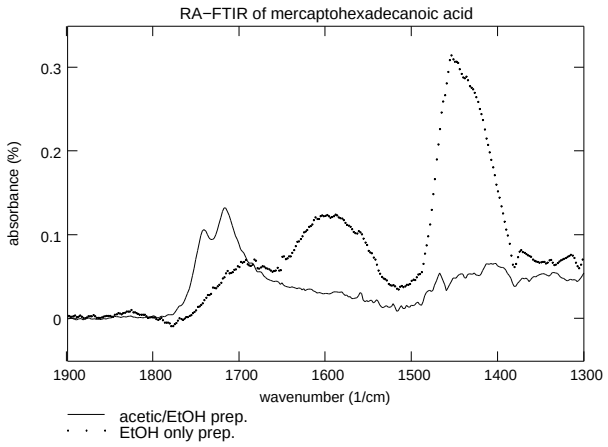

Figure 4: Reflection-Absorption Fourier Transform Infrared Spectra of a mercaptohexadecanoic acid monolayers formed with acetic acid in solution and monolayers formed with only ethanol as the solvent.

much larger, while one associated with water (1600cm^{-1}) also appears. This indicates that the ethanol-only sample carboxyl groups exist as highly dimerized pairs and carboxylates.

Sulfur photoelectron spectra were used to determine attachment of the molecules to the substrate. Monolayers formed with carboxyl terminated alkanethiols were never completely free of unbound thiol. There is a dependence of the relative intensities vs. concentration as shown in figure 5 The percentage of unbound thiol is estimated using a mean free path of electrons of 5.5Å for this kinetic energy range and material.[20–23] There is a slight decrease in unbound sulfur with decreasing concentration. This occurs for two reasons: There is a higher relative concentration of acetic acid to mercaptohexadecanoic acid in the solution, and there is hydrogen bonding in the molecules, and a molecule hydrogen bound to acetic acid rather than another long alkyl chain molecule will be more accessible to the surface, especially at lower concentration (kinetic effects). The improved film at lower concentration also indicates that this film is most likely closest to a true monolayer of molecules. In the ethanol only sample, a large unbound intensity concentration indicates that there are many unbound molecules in this sample and that using only ethanol for the formation and rinsing of the SAM is not sufficient to form a true monolayer.

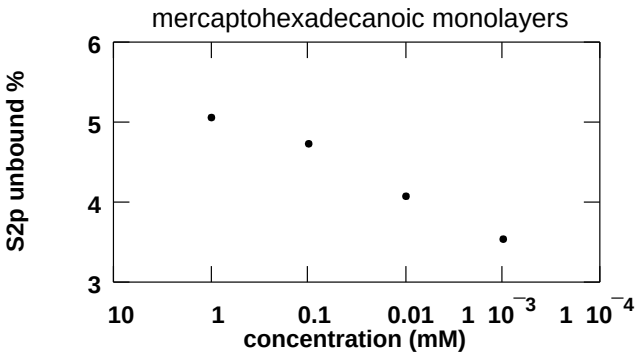

Figure 5: The percentage of unbound thiol intensity in the S2p spectra measured with hν=280eV. Unbound thiol increases with increasing concentration.

4 Conclusions

The various conformations of carboxyl-terminated alkylthiols are summarized in figure 6. Well-ordered, carboxyl terminated self-assembled monolayers of mercaptohexadecanoic acid on Au(111) can be formed by adding acetic acid to the ethanol solution. This paper conclusively shows well ordered films measured using NEXAFS, complimenting recent FTIR results.[9] Carbon K-edge absorption features reveal an alkyl chain ordered upright to the surface and tilted about 39 degrees from normal. In addition, the carboxyl group normal is tilted about 45 degrees from the surface normal, and this is confirmed with analysis of the Oxygen K-edge π^* and σ^* features. Molecules not bound to the surface (3-5%) exist in the layers, and are not expected to significantly effect NEXAFS results. This ratio of unbound sulfur to bound sulfur decreases with decreasing concentration. The decrease is due to the higher relative concentration of acetic acid to the molecules in solution ensuring protonated carboxyl endgroups, and due to higher accessibility of the single molecules to the surface compared to large long-chain molecules dimerized to each other.

When carboxyl-terminated alkyl-thiols are adsorbed on gold from the commonly used method of dissolving the molecules in ethanol, Carbon K-edge absorption spectra reveal a monolayer that shows less order within the alkyl chains. C K-edge NEXAFS also has little polarization dependence in the carboxyl π^* peak which indicates nearly randomly oriented carboxyl groups. FTIR spectra and C1s photoemission indicate that much of the endgroups are actually carboxylate, while S2p photoemission show a large fraction of unbound molecules on the surface. Electro-

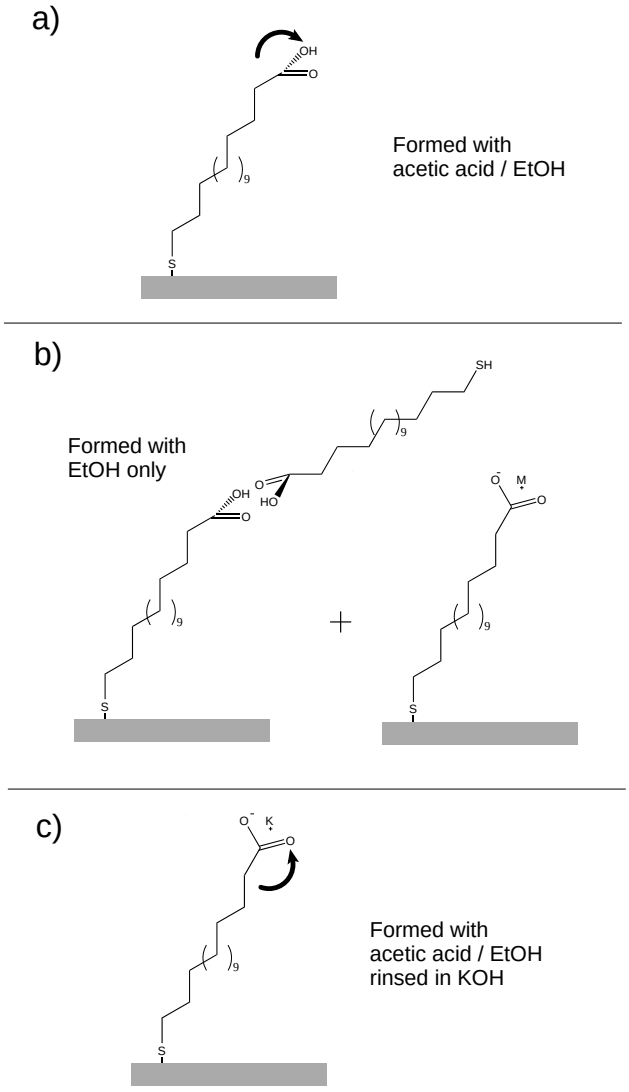

Figure 6: Schematic representation of orientation of terminating endgroup of mercaptohexadecanoic acid on gold. a) Formed with acetic acid. b) Formed in ethanol only. c) Monolayer formed with acetic acid, but then rinsed in KOH solution.

statically charged endgroups and dimerized pairs of molecules hinder SAM formation in this case.

A stark conformational change occurs in the carboxyl group of well-formed monolayers upon exposure to non-volatile basic solutions. Here, exposure to KOH causes the carboxyl group to be oriented much more upright, indicating carboxyl group orientation chemical switchability within these films. Carbon and Oxygen K-edge spectra indicate the normal to the carboxyl group plane changes from an average of 45 degrees to about 65 degrees.

Acknowledgments: The authors thank the SSRL staff, especially Curtis Troxel and Jan Luning for assistance during these experiments. Also thanks to Mark Engelhard and Don Baer at the Environmental Molecular Science Laboratory, Pacific Northwest National Laboratory, for preliminary XPS spectra in this work, and Cheryl Evans, LLNL, for additional XPS spectra confirming synchrotron results. Also thanks to C. Wöll, Univ. Bochum, Germany for useful discussions on these films. This work was performed under the auspices of the U. S. Department of Energy by University of California Lawrence Livermore National Laboratory under Contract W-7405-ENG-48. Work was conducted at the Stanford Synchrotron Radiation Laboratory, which is supported by the U.S. Department of Energy under contract DE-AC03-76SF00515. Supporting Information Available: C K-edge total electron and auger yield absorption, O K-edge auger yield absorption, C1s X-ray photoelectron, S2p X-ray photoelectron spectra are available for all samples. Also, example regression plots and all derived NEXAFS angles and errors are presented in the supporting information. This material is available free of charge via the Internet at http://pubs.acs.org.

References

1. Vance, A. L.; Willey, T. M.; van Buuren, T.; Nelson, A. J.; Bostedt, C.; Fox, G. A.; Terminello, L. J. *Nano Letters* **2003,** *3,* 81-84.

2. Vance, A. L.; Willey, T. M.; Nelson, A. J.; van Buuren, T.; Bostedt, C.; Terminello, L. J.; Fox, G. A. *Langmuir* **2002,** *18,* 8123-8128.

3. Patel, N.; Davies, M. C.; Hartshorne, M.; Heaton, R. J.; Roberts, C. J.; Tendler, S. J.; Williams, P. M. *Langmuir* **1997,** *13,* 6485-6490.

4. Patel, N.; Davies, M.; Heaton, R.; Roberts, C. J.; Tendler, S. J. B.; Williams, P. M. *Applied Physics A, Materials Science and Processing* **1998,** *66,* S569-S574.

5. Lahann, J.; Mitragotri, S.; Tran, T.-N.; Kaido, H.; Sundaram, J.; Choi, I. S.; Hoffer, S.; Somorjai, G. A.; Langer, R. *Science* **2003,** *299,* 371-374.

6. Nuzzo, R. G.; Dubois, L. H.; Allara, D. L. *Journal of the American Chemical Society* **1990,** *112,* 558-569.

7. Dannenberger, O.; Weiss, K.; Himmel, H. J.; Jäger, B.; Buck, M.; Wöll, C. *Thin Solid Films* **1997,** *307,* 183-191.

8. Himmel, H.-J.; Weiss, K.; Jäger, B.; Dannenberger, O.; Grunze, M.; Wöll, C. *Langmuir* **1997,** *13,* 4943-4947.

9. Arnold, R.; Azzam, W.; Terfort, A.; Wöll, C. *Langmuir* **2002,** *18,* 3980-3992.

10. Hydrogen flame annealing follows the method described by Molecular Imaging, http://www.molec.com.

11. Tirsell, G. K.; Karpenko, V. P. *Nucl. Instrum. Methods* **1990,** *A291,* 511-517.

12. Zharnikov, M.; Grunze, M. *Journal of Vacuum Science and Technology B* **2002,** *20,* 1793-1807.

13. Batson, P. E. *Physical Review B* **1993,** *48,* 2608-2610.

14. Stöhr, J.; Outka, D. A. *Physical Review B* **1987,** *36,* 7891-7904.

15. Stöhr, J. *NEXAFS Spectroscopy;* Springer Verlag: Berlin Heidelberg, 1992.

16. Bagus, P.; Weiss, K.; Schertel, A.; Wöll, C.; Braun, W.; Hellwig, C.; Jung, C. *Chemical Physics Letters* **1996,** *248,* 129-135.

17. Hanher, G.; Kinzler, M.; Wöll, C.; Grunze, M. *Physical Review Letters* **1991,** *67,* 851-854.

18. Heister, K.; Johansson, L. S.; Grunze, M.; Zharnikov, M. *Surface Science* **2003,** *529,* 36-46.

19. Smith, E. L.; Alves, C. A.; Anderegg, J. W.; Porter, M. D. *Langmuir* **1992,** *8,* 2707-2714.

20. Powell, C. J.; Jablonski, A. *NIST Electron Effective-Attenuation-Length Database - Version 1.0;* National Institute of Standards and Technology, Gaithersburg, MD: , 2001.

21. Powell, C. J.; Jablonski, A. *NIST Electron Inelastic-Mean-Free-Path Database - Version 1.1;* National Institute of Standards and Technology, Gaithersburg, MD: , 2001.

22. Laibinis, P. E.; Bain, C. D.; Whitesides, G. M. *Journal of the American Chemical Society* **1991,** *95,* 7017-7021.

23. Lamont, C. L. A.; Wilkes, J. *Langmuir* **1999,** *15,* 2037-2042.

Supplemental Information

Chemically Transformable Configurations of Mercaptohexadecanoic Acid Self-Assembled Monolayers Adsorbed on Au(111)

T. M. Willey, A. L. Vance, et al.

January 13, 2004

Carbon absorption spectra for samples investigated are presented in figure 1. Auger yield has higher surface sensitivity, and this can easily be seen in the fact that the carboxyl feature is much more intense than total-electron yield. It is interesting to note that the polarization dependence disappears much more in the EtOH only sample in auger yield, which indicates the SAM is more disordered near the vacuum interface. This may also arise due to the many unbound molecules decorating the surface seen in the S 2p photoemission spectra.

Figure 2 presents the output from simultaneously fitting spectra from 6 different incidence angles (90^o = normal) and all unique difference spectra. Peak positions and widths are held constant across all spectra, while amplitudes are allowed to vary independently in every spectra.

Figure 3 is an example of linear regressions from the R* in the 0.001 mmol sample using ratios of intensities. Lines using the intensity at 20^o - 70^o in the denominator of the equations described in the article text result in two angles: one from the slope, and one from the offset at $\cos^2\theta = 0$. For the intensity at 90^o, only the slope returns a value. These results from the 0.001 mmol sample are listed in table 1. The average of all 11 values is used as the angle, while the standard deviation is reported as the error. These values for all samples and resonances are

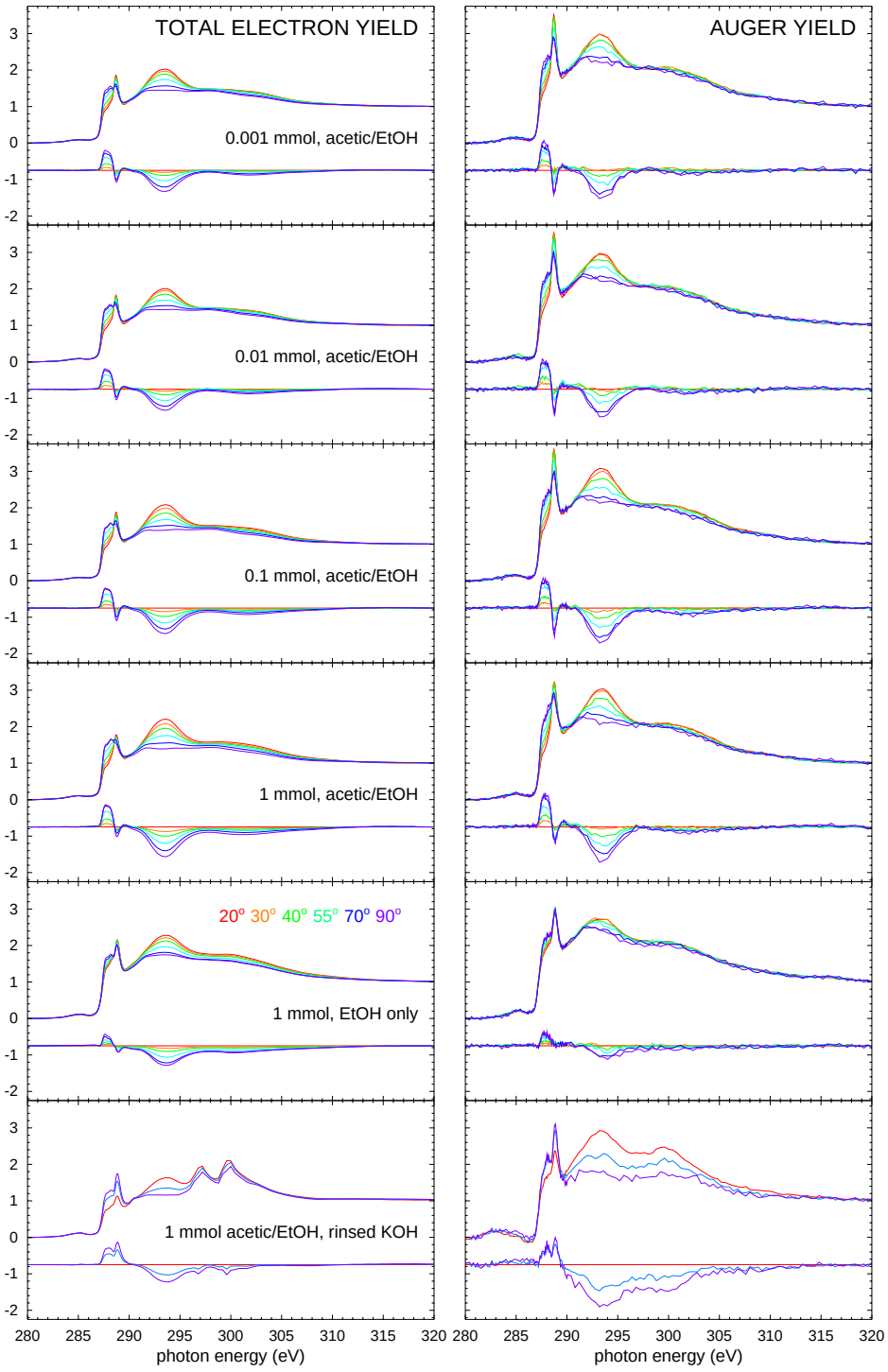

Figure 1: Carbon K-edge absorption spectra.

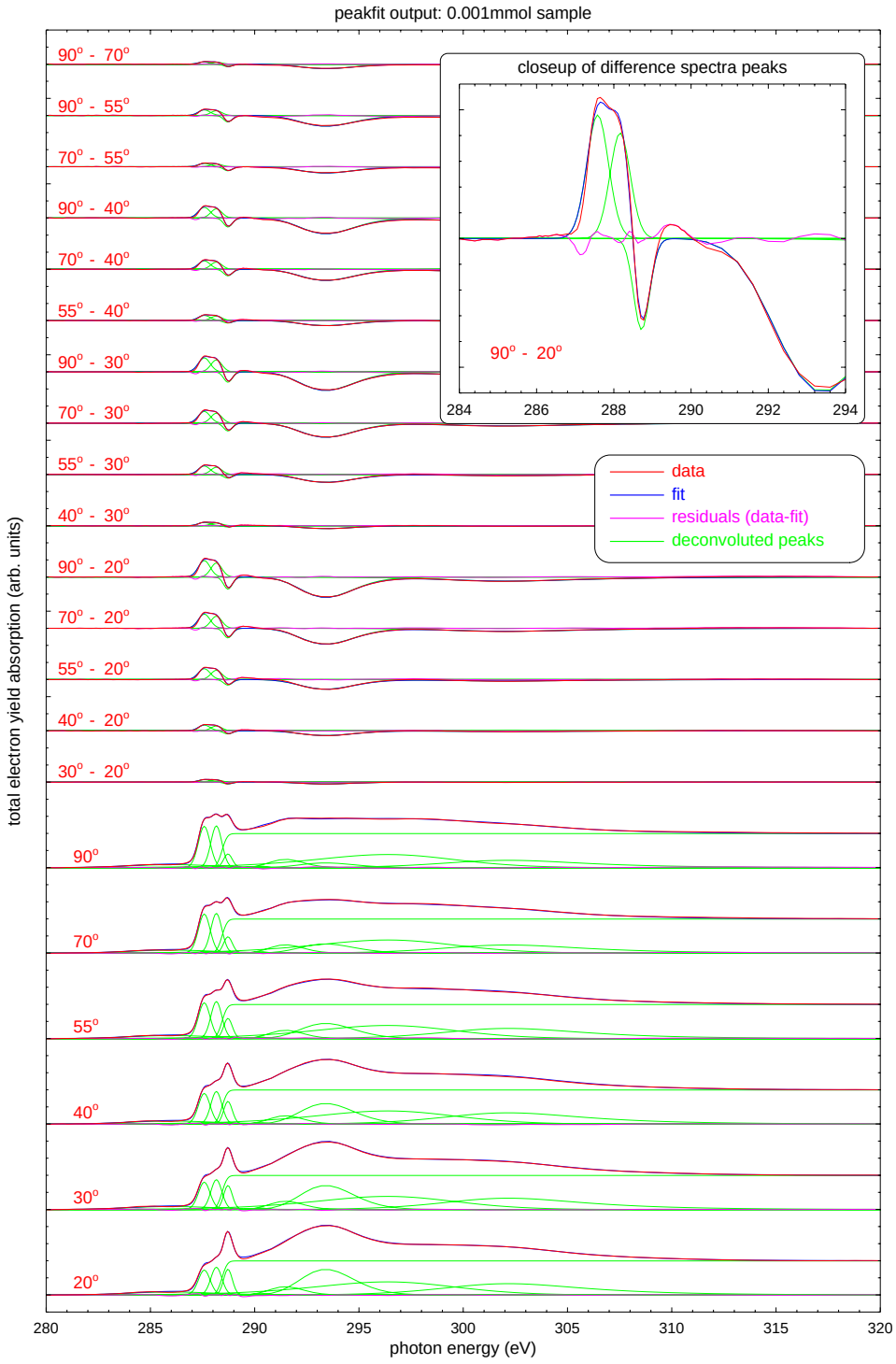

Figure 2: An example of simultaneous fit of Carbon K-edge raw and difference spectra.

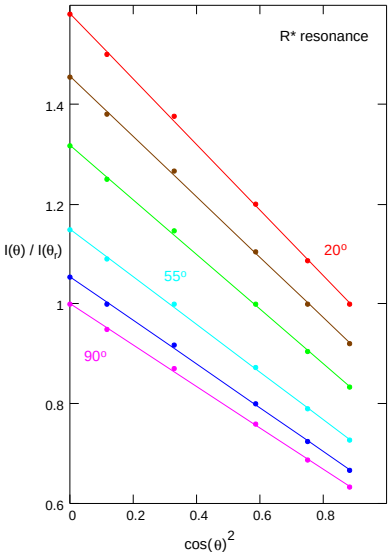

Figure 3: Linear regression of feature intensities divided by angle (color) vs. cosine squared for the 0.001 mmol sample.

presented in table 2. The values in 3 were computed in a similar manner.

The second method for determining orientation of bonds is through difference spectra, which isolate polarization dependent resonances. Figure 4 demonstrates the linear regression from the R* region in the 0.001 mmol sample using all combinations of difference spectra vs. $\cos^2\theta_i - \cos^2\theta_j$. For this method, the difference between the value returned by the linear regression and one of the 95% upper or lower confidence line slopes is used for the error. These error values are for precision and do not represent a number of other sources of systematic errors such as the experimental setup sample manipulator to incidence beam alignment, the model of a transition-dipole-moment as a vector rather than an orbital with three-dimensional structure, innaccuracies in peakfitting the resonances and absorption step, or a distribution of angles within the samples pushing the measurement towards the magic angle of 54.7^o. Of particular interest, constraining the main absorption step edge to various energies from 288.2 to 288.8eV results in little change to the computed carboxyl tilt angle as the carboxyl resonance lies very near the absorption step of the alkyl-chain. We estimate with consideration of these sources of uncertainty that our measurements are accurate to about 4-5^o. The paper mentions that the carboxyl orientation is not due to odd even effects. Figure 6

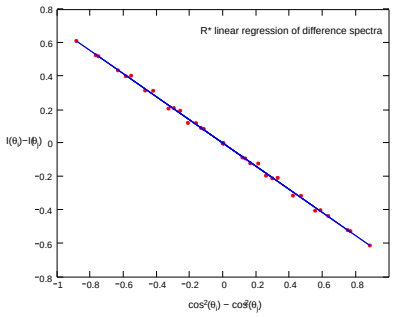

Figure 4: Linear regression of all difference spectra feature intensities for the R* region of the 0.001 mmol sample.

Table 1: Carbon tilt angles derived from the 0.001mmol Carbon TEY spectra.

all spectra vs.:	20^o	30^o	40^o	55^o	70^o	90^o	average	std. dev.
alkyl R* slope	40.22	40.22	40.29	40.36	40.19	40.23		
alkyl R* offset	39.02	39.21	39.80	40.72	38.89			
both slope and offset							39.92	0.58
alkyl σ* slope	40.96	41.63	42.13	42.91	41.52	40.83		
alkyl σ* offset	42.32	41.77	41.15	38.96	42.91			
both slope and offset							41.55	1.06
carboxyl π* slope	44.65	44.59	45.04	45.46	44.85	44.35		
carboxyl π* offset	45.06	45.20	44.45	42.76	44.71			
both slope and offset							44.65	0.68

Table 2: Carbon tilt angles (between alkyl chain and sample normal and between the O-C=O plane normal and sample normal) for all samples.

	.001mmol	.01mmol	.1mmol	1mmol	EtOH	KOH
alkyl R*	39.9 ± .6	39.7 ± 1.0	40.0 ± 1.6	38.4 ± 1.5	48.4 ± .6	39.1 ± 2.2[b]
diff. R*	39.9[a] ± .2	40.2 ± .5	41.2 ± .5	39.8 ± .6	46.8 ± .3	[b]
alkyl σ*	41.6 ± 1.1	41.1 ± 0.9	39.1 ± .6	38.0 ± 1.2	46.9 ± .5	[b]
diff. σ*	41.6[a] ± .9	41.8 ± .7	38.2 ± .6	34.7[c] ± 1.0	36.0[a] ± .3	[b]
carboxyl π*	44.6 ± .7	45.5 ± .5	44.2 ± .9	44.5 ± 1.5	52.1 ± .3	71.6 ± 9.2[b]
diff. π*	44.6[a] ± .6	45.0 ± .5	43.8 ± .5	44.9 ± .9	48.6 ± .3	[b]

[a] used as reference for difference spectra
[b] high uncertainty or unavailable due to K photoelectron peaks in spectral window.
[c] diff. σ* underestimates tilt due to thicker layers in 1mmol, EtOH samples

Table 3: Oxygen tilt angles (between the O-C=O plane normal and sample normal) for all samples.

	.001mmol	.01mmol	.1mmol	1mmol	EtOH	KOH
π*	45.2 ± .4	44.6 ± .2	44.5 ± .2	46.7 ± .2	51.9 ± .2	63.6 ± .6
diff. π*	45.2[b] ± .6	44.8 ± .2	45.4 ± .3	44.7 ± .3	51.0 ± .3	65.5 ± 1.7
σ*	41.6 ± .3	43.3 ± .5	40.0 ± .7	45.4 ± .6	50.8 ± .2	[a]
diff. σ*	41.6[b] ± .6	43.5 ± 1.4	39.3 ± 1.8	45.6 ± 2.1	51.4 ± 1.5	[a]

[a] σ* not available on KOH rinsed sample due to K photoelectron peaks

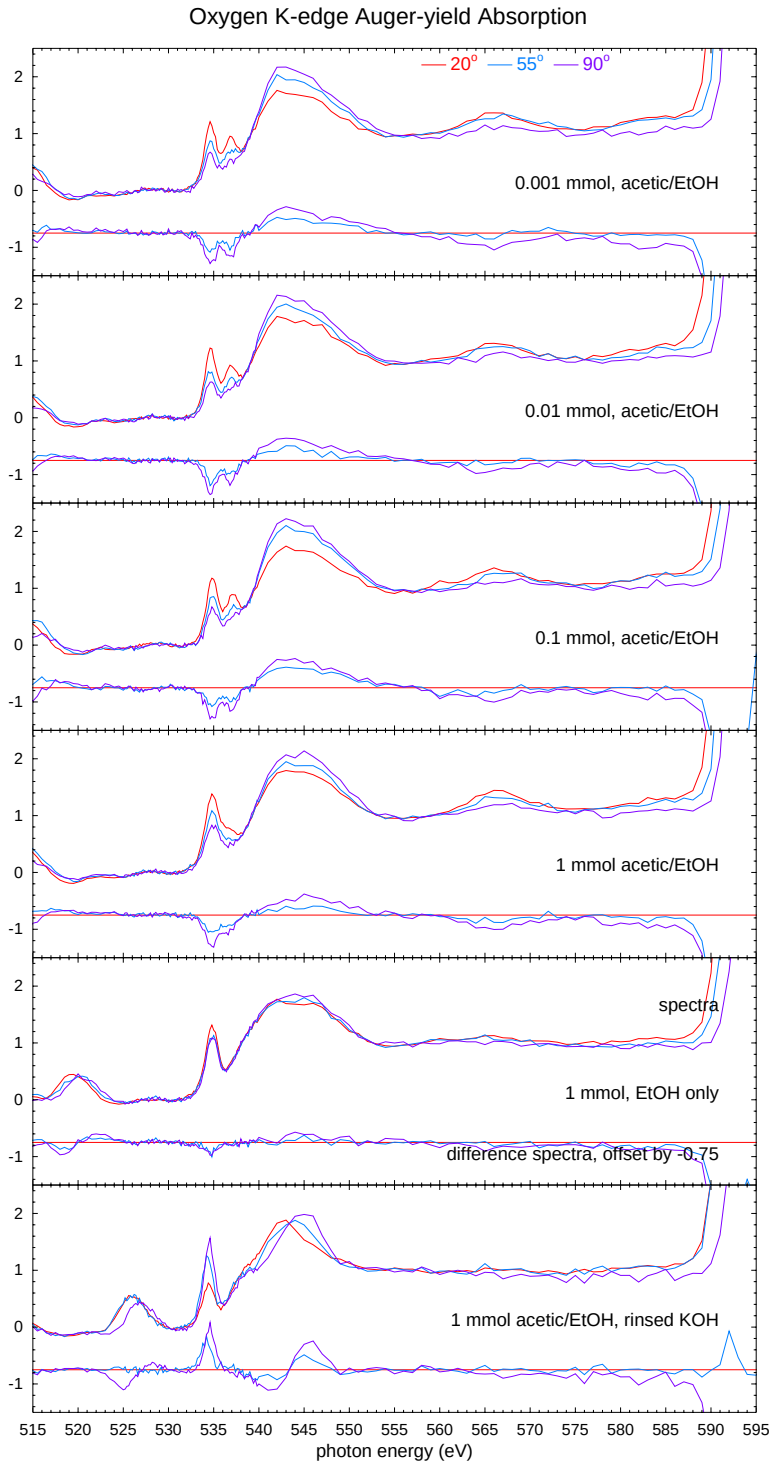

Figure 5: Oxygen K-edge auger-electron yield absorption spectra.

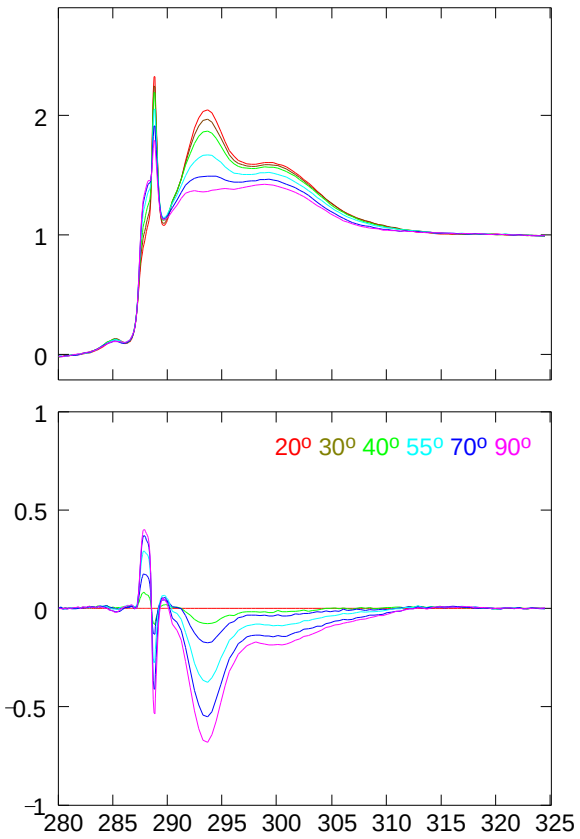

Figure 6: Carbon K-edge NEXAFS for mercaptoundecanoic acid SAM, showing carboxyl polarization dependence is not an odd-even effect.

presents the NEXAFS from mercaptoundecanoic acid. This molecule showed orientation very similar to that of the mercaptohexadecanoic acid with angles presented in the paper.

It should also be noted that if acetic acid was not used in the solution of formation, and the samples were only rinsed in ethanol, large amounts of ions were seen on the surface. This is also indicated in carbon photoemission spectra in the paper showing a mixture of carboxyl and carboxylate terminations in this case. Rinsing SAMs in ultra pure (milliQ) resulted in fewer ions, but occasionally one could still see trace amounts on the surfaces. Rinsing the samples in acetic acid solutions consistently removed ions to below detection limits. An example is presented in figure 7: when carbon absorption scans are extended to include the Calcium L-edge (excitation from Ca 2p electronic states) one sees a large intensity of Ca when rinsed in EtOH only. Water also can leave trace amounts of Ca; the scan

in this figure is one of the best we encountered when rinsing with water only, but it still contains Ca peaks. Rinsing in acetic solutions removes Ca to below the detection limit. It is also interesting to note that in initial samples, a reasonably high degree of order was seen in samples produced and rinsed with only EtOH as the solvent. This was highly irreproducible, and generally samples were less ordered than those formed subsequently with acetic acid in solutions. Also, these initial samples consistently had a larger C1s signal than similar length methyl terminated SAMs, and consistently had large amounts of unbound thiol. We speculate that bilayer formation may have played a role in some of these samples and in their appearing more ordered.

Carbon 1s photoelectron spectra, best fits using simple gaussians and error functions for backgrounds, deconvoluted gaussian peaks, and residuals are presented in figures 8 - 13. The higher binding energy peak is sharp and at its highest energy when prepared using acetic acid in EtOH solvents with molecules as protonated carboxyl groups. The two-component fit of the alkyl peak shows the asymmetry in this peak, and may be due to either alkyl carbon atoms near the carboxyl functionalization, or may be effects seen by Heister et al. as described in the article text. In samples prepared with EtOH only, the high energy peak shifts to lower binding energy and broadens significantly, indicating many different states of the carboxyl/carboxylate group of the molecule. There is also much larger asymmetry of the alkyl peak with more intensity to the high binding energy side. For the SAM that has been rinsed in KOH, once again the high energy peak is very sharp, but now at much lower binding energy as carboxylate. The alkyl peak has not only shifted to higher energy, but the asymmetry is now very different, with the sharpest rise on the high binding energy side.

Figures 17 - 19 present Sulfur 2p spectra, best fits, and residuals. Gaussians and error functions were again used to fit the spectra, with an $S2p_{3/2}$ to $S2p_{1/2}$ branching ratio of about 2:1 and a difference in binding energy of about 1.2eV. Bound thiolate had components $S2p_{3/2}$ and $S2p_{1/2}$ at about 161.95eV and 162.14eV. Unbound thiol had components at about 163.45eV and 164.65eV. The EtOH only sample has two unbound peaks; the lower and more intense peak is most likely disulfide that has formed in an unknown manner. The trend presented in the text of increasing unbound with increasing molecular concentration in the solution the SAM was formed in is visible in

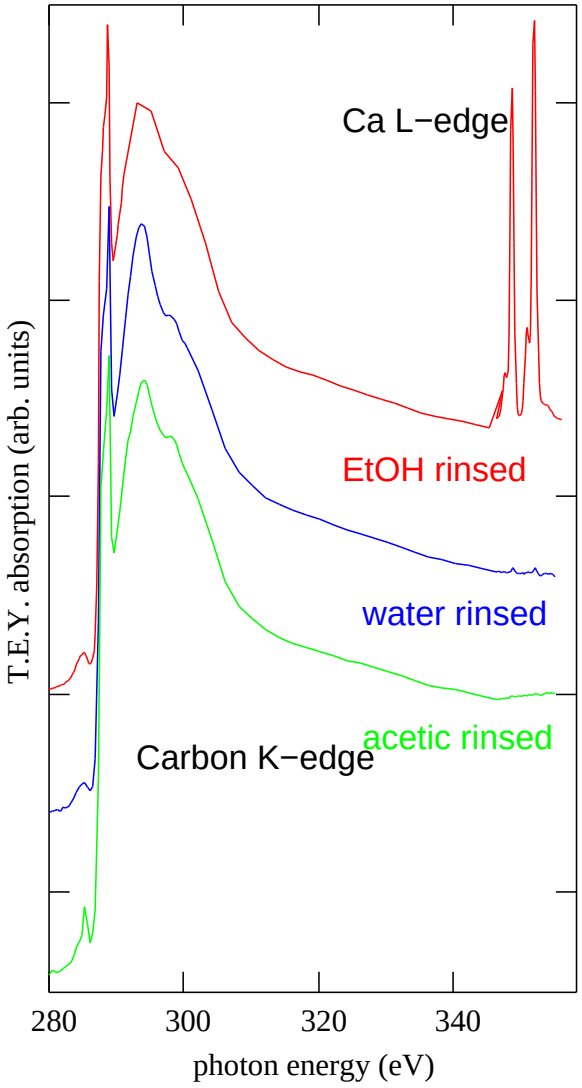

Figure 7: Spurious ions often left on sample when not rinsed in acetic acid. Top: ethanol only rinse. Middle: water rinse. Bottom: acetic acid solution rinse.

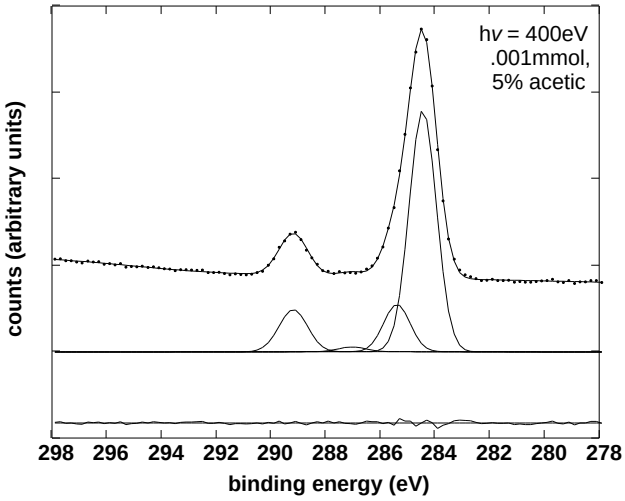

Figure 8: Carbon C1s taken at a photon energy of 400eV for the .001mmol in 5% acetic acid / ethanol sample. Spectra (dots) + best fit, individual peaks within the fit, and residuals (data - best fit) are presented.

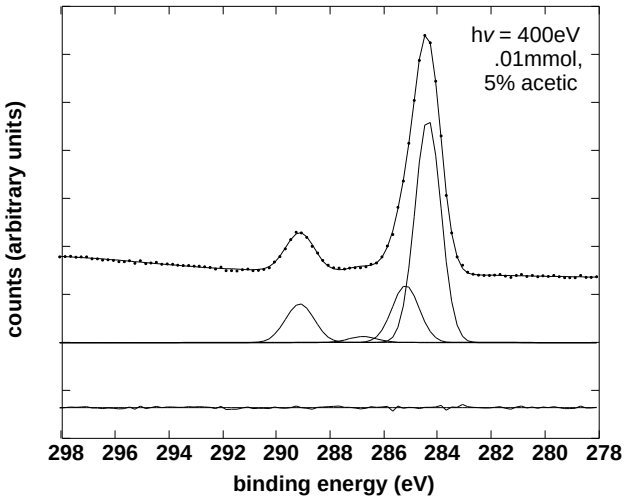

Figure 9: Carbon C1s taken at a photon energy of 400eV for the .01mmol in 5% acetic acid / ethanol sample. Spectra (dots) + best fit, individual peaks within the fit, and residuals (data - best fit) are presented.

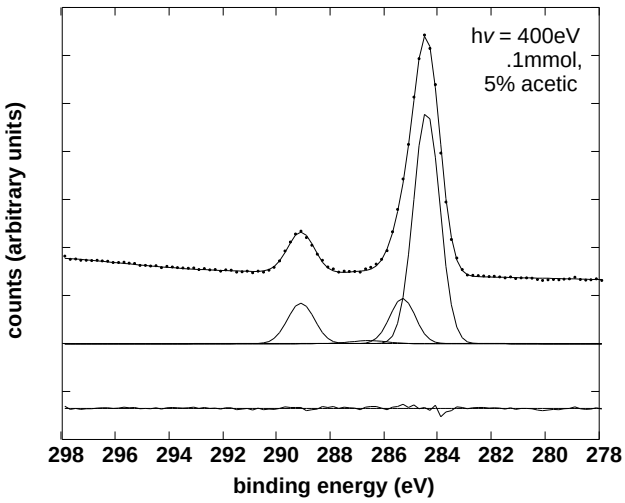

Figure 10: Carbon C1s taken at a photon energy of 400eV for the .1mmol in 5% acetic acid / ethanol sample. Spectra (dots) + best fit, individual peaks within the fit, and residuals (data - best fit) are presented.

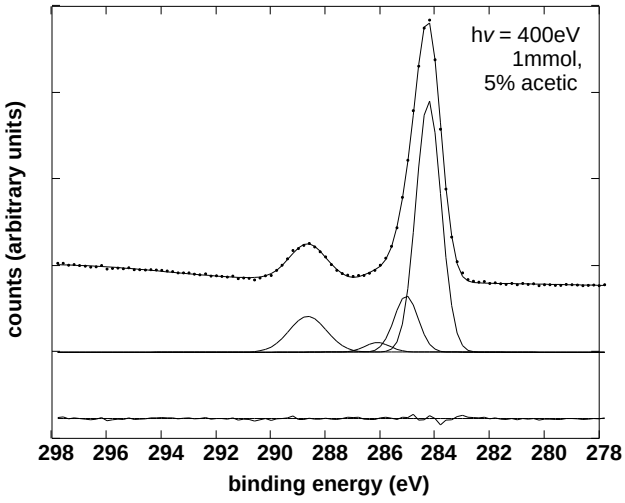

Figure 11: Carbon C1s taken at a photon energy of 400eV for the 1mmol in 5% acetic acid / ethanol sample. Spectra (dots) + best fit, individual peaks within the fit, and residuals (data - best fit) are presented.

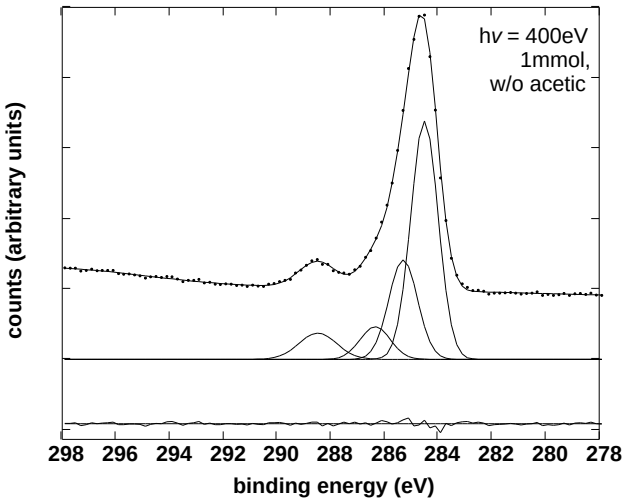

Figure 12: Carbon C1s taken at a photon energy of 400eV for the 1mmol in ethanol only sample. Spectra (dots) + best fit, individual peaks within the fit, and residuals (data - best fit) are presented.

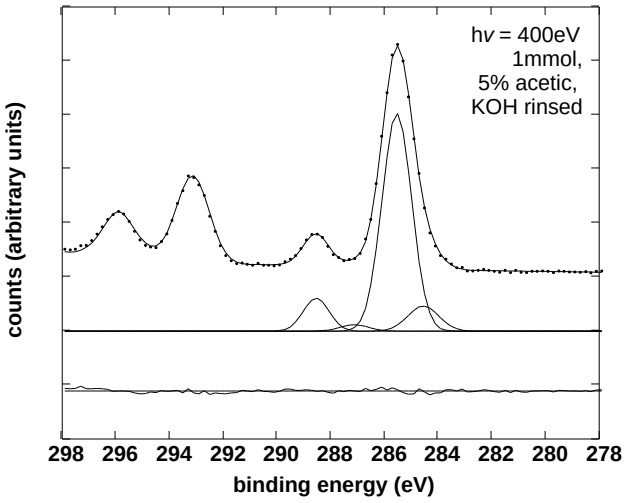

Figure 13: Carbon C1s taken at a photon energy of 400eV for the 1mmol in 5% acetic acid / ethanol, rinsed in KOH sample. Spectra (dots) + best fit, individual peaks within the fit, and residuals (data - best fit) are presented.

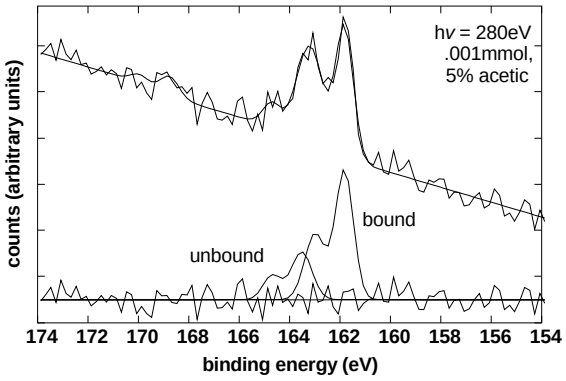

Figure 14: Sulfur 2p taken at a photon energy of 280eV for the 0.001mmol in 5% acetic acid / ethanol sample. Spectra + best fit, individual spin-orbit split components within the fit, and residuals (data - best fit) are presented.

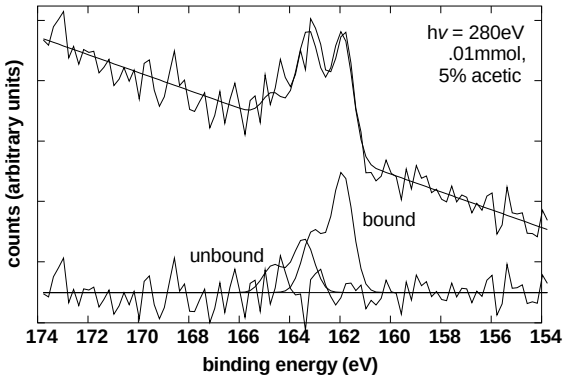

Figure 15: Sulfur 2p taken at a photon energy of 280eV for the 0.01mmol in 5% acetic acid / ethanol sample. Spectra + best fit, individual spin-orbit split components within the fit, and residuals (data - best fit) are presented.

these spectra. Results for the KOH rinsed sample are more noisy due to shorter acquisition time. Unlike methyl terminated SAMs, we were unable to completely remove unbound thiol and disulfide.

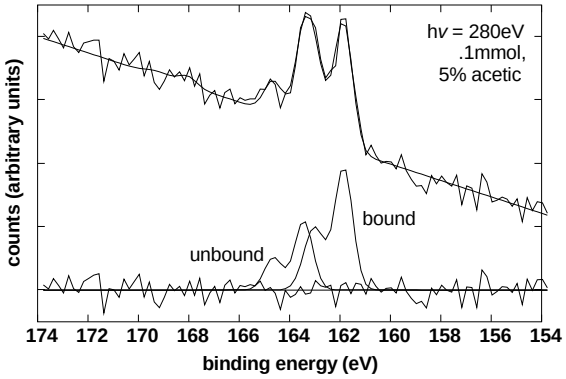

Figure 16: Sulfur 2p taken at a photon energy of 280eV 0.1mmol in 5% acetic acid / ethanol sample. Spectra + best fit, individual spin-orbit split components within the fit, and residuals (data - best fit) are presented.

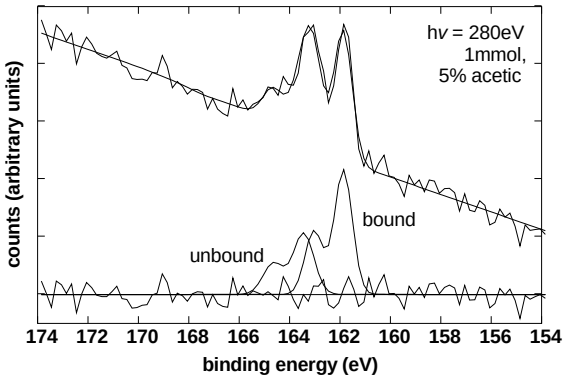

Figure 17: Sulfur 2p taken at a photon energy of 280eV for the 1mmol in 5% acetic acid sample. Spectra + best fit, individual spin-orbit split components within the fit, and residuals (data - best fit) are presented.

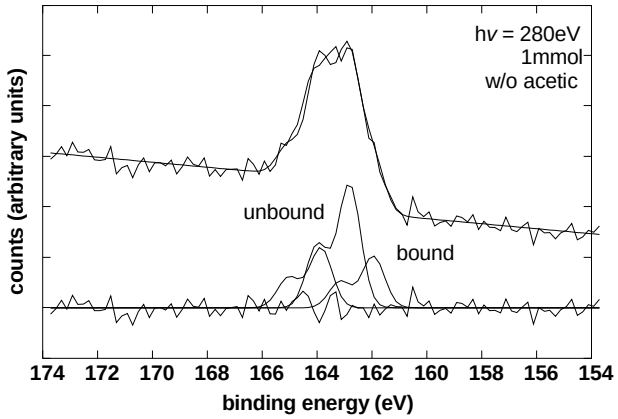

Figure 18: Sulfur 2p taken at a photon energy of 280eV for the 1mmol formed in ethanol only.

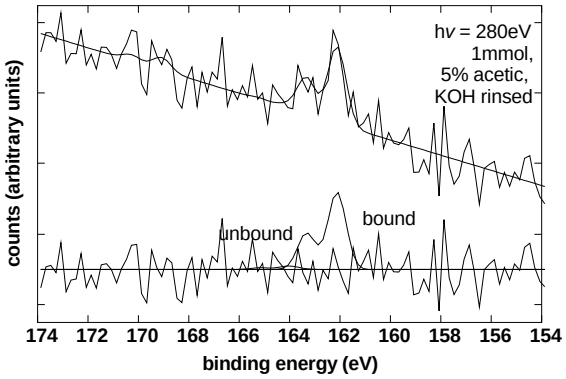

Figure 19: Sulfur 2p taken at a photon energy of 280eV for the 1mmol in 5% acetic acid sample that was rinsed in KOH.